Design and Structural Parameter Optimization of Airborne Horticultural Multi-DOF Manipulator

Changgao Xia[1], Chenxi Sun[1,*], and Jiangyi Han[1]

[1] College of Automotive and Traffic Engineering, Jiangsu University, Zhenjiang 212013, P.R. China
[*] Corresponding author. E-mail: scx0663@163.com

Received: Feb. 26, 2020, Accepted: May. 15, 2020

In order to improve the quality and efficiency of hedge trimming, a research of a four-degree-of-freedom trimming manipulator is carried out in this paper. The global kinematic performance metric (that is, the Global Condition Index constructed by the Jacobian matrix) is utilized to measure the dexterity of the manipulator. Then the structural parameter optimization model is established using the maximum Global Condition Index(GCI) as the objective function and the particle swarm algorithm is used to solve the optimization problem. The optimal link lengths(big arm, middle arm forearm) of the manipulator are 1190, 937, and 633mm, the initial GCI is 0.68442, and the optimized value is 0.79521. Obviously, the dexterity is higher. To verify the feasibility of the optimized manipulator, this paper proposes a method to evaluate the workspace, using accessibility to express how much the actual workspace satisfies the target workspace. Simulation results show that the reachability of optimized manipulator is 100%, improved by 11.21%, which proves that the optimized manipulator is completely feasible.

Keywords: Trimming manipulator; Global Condition Index; optimization; workspace

http://dx.doi.org/10.6180/jase.202009_23(3).0017

1. Introduction

Hedges are the barriers of orchards, which play a role of separation and protection, making full use of natural resources, maintaining the ecological environment, beautiful and environmentally friendly. However, the trimming of hedges is very tedious. Nowadays, it is widely used handheld hedge trimmers, but this kind of trimming by handheld tool of green personnel has many disadvantages, not only more pollution, but also low work efficiency. Therefore, the development of automatic trimming manipulators has become a hot spot, and the research of hedge trimming manipulators has important practical significance for improving the level of environmental greening equipment.

At present, the existing industrial manipulators are bulky, costly, and not suitable for hedge trimming. However, there are few researches on hedge trimming manipulators. Jinan Jinli Company has produced a vehicle-mounted hedge trimmer, which has greatly improved efficiency compared with manual trimming, but it has a heavy structure and inflexible movement [1]. Most of the current manipulators have such problems, so many scholars have proposed some optimization methods. Wang [2] proposed to optimize the volume of the manipulator's upper and lower arms. Wang et al. [3] took the optimal envelope surface of the main section of the manipulator's workspace as the objective function. Tian et al. [4] took the volume of the workspace as the optimization goal, and adopted the adaptive meshing method for optimization. In addition, Salisbury [5] used the condition number of Jacobian matrix as an optimization parameter, and the closer the condition number is to 1, the better the isotropy of the manipulator, but this is only a local metric and cannot represent global performance. In view of the above problems, this paper designs a trimming manipulator and optimizes its structural parameters to improve the dexterity of the manipulator. The "Global Condition Index" (GCI) proposed by Gosselin and Angeles [6] is selected as the optimization index, and the particle swarm algorithm is adopted to solve the optimization problem to obtain the optimal link lengths.

This paper also proposes a method to evaluate the

workspace to verify feasibility of the optimized manipulator. Plenty of literature uses numerical methods [7–9] to evaluate the workspace of the manipulator. Pond and Carretero [10] proposed to evaluate the workspace based on the condition number of the Jacobian matrix. Qu et al. [11, 12] used the search method to draw a three-dimensional map of the manipulator's workspace point by point in the Cartesian coordinate system. Tsai et al. [13–15] calculated the workspace by Monte Carlo method in the joint space, and Chaudhury proved the feasibility of this method through two examples. In summary, the Monte Carlo method is the more common method for evaluating workspace. Most scholars apply it to joint space, which is relatively simple, but not intuitive. Different from them, this paper uses Monte Carlo method in the operating space, first, randomly generate 3D coordinate points to obtain the target workspace, then substitute these points into the inverse kinematics to generate the actual workspace based on the limitation of the joint angle ranges. The reachability is used to express the degree to which the actual work space satisfies the target workspace, only when the reachability is 100%, the manipulator is fully feasible.

2. Structural Design of the Manipulator

The degree of freedom is an important technical index of the manipulator, which is determined by its structure and directly affects its maneuverability [16]. Too many degrees of freedom, the manipulator moves flexibly, but may produce redundant degrees of freedom, complex structure, and difficult to control; Too few degrees of freedom, it cannot complete the specified action [17]. Wei [18] designed a 5-DOF trimming manipulator, including lifting, retracting, and rotating mechanisms, with flexible motion, but its kinematic model was too complicated to control. Li [19] and Fu [20] designed 3-DOF manipulators respectively, the former is a planar manipulator; The latter is a spatial manipulator, but only two joints can be controlled to reach the goal position. In this paper, the manipulator belongs to the on-board device of a tractor, and its function is to trim the top and sides of the hedges within a range of 1-2 meters high and 0.8 meters wide. Obviously these 3-DOF manipulators cannot complete the trimming task and very inflexible. In order to meet the trimming requirements and keep the structure simple, the prismatic joint is not considered, and a 4-DOF trimming manipulator (as shown in Fig. 1) is adopted, which is the simpler and more easily controlled model in the manipulators that can meet the trimming requirement. The trimming manipulator is installed at the front of the tractor, the driver drives the tractor at a constant speed to trim the hedges, the workspace of the manipulator is a cuboid with length, width and height of a, b and h, respectively.

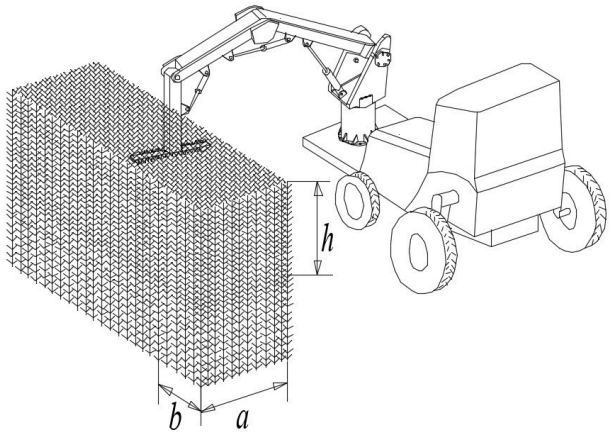

Fig. 1. 4-DOF manipulator trimming structure.

The four joints of the manipulator are rotary joints, the first joint can rotate 360^0 to realize the trimming of any plane in the space, the other joints can rotate within certain ranges, as shown in Table 1. By controlling their joint angles, they can reach any point in the operating space. The end- effector of the manipulator is a trimming tool.

Table 1. Joint motion range.

Joint Number	Motion Range(Degree)
1	0∼360
2	0∼180
3	-120∼0
4	-120∼60

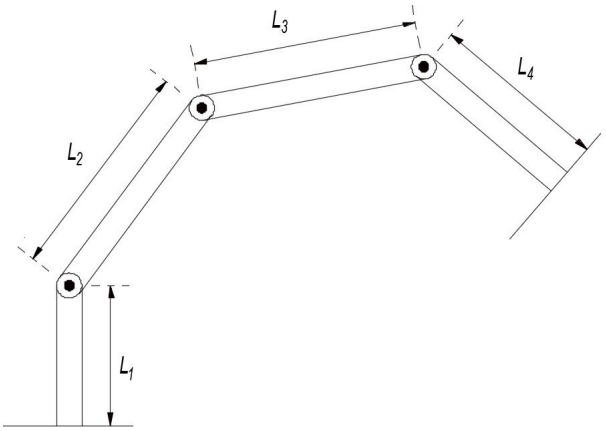

Fig. 2. Simplified structure of 4-DOF manipulator.

The simplified structure of the 4 -DOF trimming manipulator is shown in Fig. 2 L_1, L_2, L_3, L_4 are the link lengths

of the swing arm, big arm, middle arm and forearm, respectively. According to the tread, the height of the tractor, the distance between the inner wheel and the hedges as well as the trimming ranges, the shortest total arm length is 3060mm. Preliminary selection: $L_1 = 300\text{mm}, L_2 = 920\text{mm}, L_3 = 960\text{mm}, L_4 = 880\text{mm}$

3. Kinematic Analysis

3.1. Forward Kinematics

The Denavit-Hartenberg(D-H) convention is a well-known way to describe the kinematic of a manipulator [21]. As shown in Fig. 3, the coordinate frames are assigned based on the D-H convention, the corresponding D-H parameters are shown in Table 2. Where, θ_i is the angle between axes

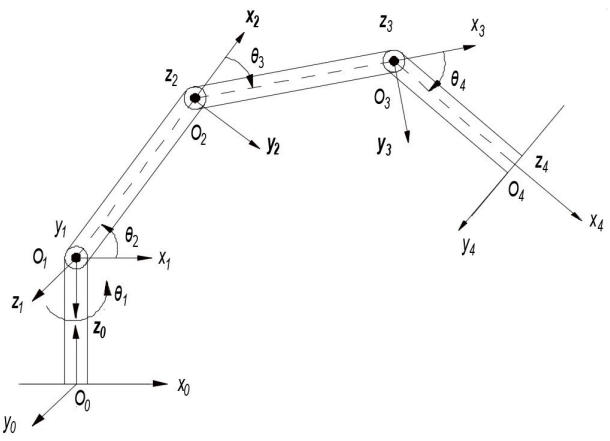

Fig. 3. Setting of the 4-DOF manipulator coordinate system.

Table 2. D-H link parameters.

Joint	Link Parameters			
	α_i	d_i	a_i	θ_i
1	π / 2	L_1	0	θ_1
2	0	0	L_2	θ_2
3	0	0	L_3	θ_3
4	0	0	L_4	θ_4

x_{i-1} and x_i at about z_{i-1}; α_i is the angle between axes z_{i-1} and z_i at about x_i; a_i is the distance between axes z_{i-1} and z_i along x_i; d_i is the distance between axes x_{i-1} and x_i along z_{i-1}.

The forward kinematics equation of the manipulator is as follows

$$T_4^0 = T_1^0 \cdot T_2^1 \cdot T_3^2 \cdot T_4^3 = \begin{bmatrix} n_x & s_x & a_x & p_x \\ n_y & s_y & a_y & p_y \\ n_z & s_z & a_z & p_z \\ 0 & 0 & 0 & 1 \end{bmatrix} = \begin{bmatrix} c_1c_{234} & -c_1s_{234} & s_1 & L_4c_1c_{234} + L_3c_1c_{23} + L_2c_1c_2 \\ s_1c_{234} & -s_1s_{234} & -c_1 & L_4s_1c_{234} + L_3s_1c_{23} + L_2s_1c_2 \\ s_{234} & c_{234} & 0 & L_4s_{234} + L_3s_{23} + L_2s_2 + L_1 \\ 0 & 0 & 0 & 1 \end{bmatrix} \tag{1}$$

Where, $c_1 = \cos\theta_1, s_1 = \sin\theta_1$;
$c_{234} = \cos(\theta_2 + \theta_3 + \theta_4), s_{234} = \sin(\theta_2 + \theta_3 + \theta_4)$

3.2. Inverse Kinematics

The forward kinematics equation of this 4-DOF manipulator is:

$$T_4^0 = T_1^0(\theta_1)\, T_2^1(\theta_2)\, T_3^2(\theta_3)\, T_4^3(\theta_4) = \begin{bmatrix} n_x & s_x & a_x & p_x \\ n_y & s_y & a_y & p_y \\ n_z & s_z & a_z & p_z \\ 0 & 0 & 0 & 1 \end{bmatrix} \tag{2}$$

In this paper, algebraic method is used to solve the inverse kinematics, and the following can be obtained:

$$\theta_1 = \tan^{-1}(p_y/p_x) \tag{3}$$

$$\theta_3 = \tan^{-1}\left(\frac{\pm\sqrt{4L_2^2L_3^2 - \left(M^2 + N^2 - L_2^2 - L_3^2\right)^2}}{M^2 + N^2 - L_2^2 - L_3^2}\right) \tag{4}$$

$$\theta_2 = \tan^{-1}\left(\frac{L_2 + L_3\cos\theta_3}{L_3\cos\theta_3}\right) - \tan^{-1}\left(\frac{N}{M}\right) \tag{5}$$

$$\theta_4 = \tan^{-1}(P/Q) \tag{6}$$

Where, $M = p_z - L_1 - L_4n_z, N = p_xc_1 + p_ys_1 - L_4n_xc_1 - L_4n_ys_1$

$P = -c_1s_{23}p_x - s_1s_{23}p_y + c_{23}p_z + L_2s_3 - L_1c_{23}$,
$Q = c_1c_{23}p_x + s_1c_{23}p_y + p_z - L_3 - L_2c_3 - L_1s_{23}$

3.3. Jacobian Matrix

The Jacobian matrix is a linear transformation that maps the joint velocity into the end-effector velocity. It can be expressed as

$$\dot{x} = J(q)\dot{q} \tag{7}$$

Where, $\dot{x}$ denotes the end-effector velocity vector in the operating space, $\dot{q}$ denotes the joint velocity vector, $J(q)$ is Jacobian matrix of the manipulator.

In this paper, the first joint of the 4-DOF manipulator can rotate 360 ^{0}, so, when rotating to any plane, the end-effector velocity of the manipulator relative to the joint

velocity is fixed. Therefore, regardless of the rotation of the first joint, the Jacobian matrix can be simplified as

$$J(q) = \begin{bmatrix} -L_4 s_{234} - L_3 s_{23} - L_2 s_2 & -L_4 s_{234} - L_3 s_{23} & -L_4 s_{234} \\ L_4 c_{234} + L_3 c_{23} + L_2 c_2 & L_4 c_{234} + L_3 c_{23} & L_4 c_{234} \end{bmatrix} \tag{8}$$

4. Structural Parameter Optimization Model

4.1. Optimization Metric

Global performance metrics are widely used in robotics, namely optimization design, trajectory planning, redundancy analysis, and dexterity analysis. In this paper, the main purpose of optimizing the four-link manipulator is to obtain a higher dexterity. The Global Condition Index (GCI) proposed by Gosselin and Angeles is selected as the optimization goal. The reciprocal of the Jacobian matrix condition number $(1/k)$ is called the local condition index, and the GCI η is used to evaluate the local condition index over the entire workspace, which can prevent the optimization result from falling into a local optimum.

The condition number of the Jacobian matrix is defined as follows [22]

$$k = \|J\|\|J^{-1}\| \tag{9}$$

Where, $\|\cdot\|$ represents any norm of the matrix. J represents the Jacobian matrix, and its norm can be calculated as follows

$$\|J\| = \sqrt{tr\left(JWJ^T\right)} \tag{10}$$

Where, W is the reciprocal of the dimension of the Jacobian matrix.

The Global Condition Index is defined as

$$\eta = A/B \tag{11}$$

Where,

$$A = \int_W \left(\frac{1}{k}\right) dW \qquad B = \int_W dW$$

Where, B is the volume of the workspace, and $0 < \eta < 1$.

Using this integration to evaluate GCI will fall into the inaccuracy caused by simple averaging of $1/k$. Kumar et al. [23] randomly generated discrete points to evaluate GCI, by averaging the reciprocal of the condition numbers of all reachable points in the space, the GCI was more accurate. This paper refers to this method, but the difference is that the above needs to use inverse kinematics algorithm to convert randomly generated 3 D points into joint angles and judge whether they meet the motion ranges to determine the reachable points, so as to obtain their condition numbers and GCI, which is more complicated. In this paper, the GCI is directly obtained by randomly generating the joint angles satisfying the motion ranges.

The specific method is: first, suppose the number of cycles is N, before the start of the i^{th} cycle, randomly generate a set of joint angles that satisfy Table 1 , and calculate the reciprocal of the condition number of Jacobian matrix at this time, $1/k_i(J)$, and so on. After the N^{th} cycle, average the reciprocals of all condition numbers.

$$\eta = \frac{1}{N}\sum_{i=1}^{n} 1/k_i(J) \tag{12}$$

In order to maximize the dexterity of the manipulator, the GCI should be maximized when the constraints are satisfied. Therefore, the objective function of this paper is

$$F(X) = \max(\eta) \tag{13}$$

4.2. Determination of Optimization Design Variables

The design variables of the trimming manipulator mainly include L_1, L_2, L_3, L_4. since L_1 is only related to the trimming height and does not affect the dexterity, it is not considered as a design variable. So, the variable is $X = [L_2, L_3, L_4]$. In order to reduce the complexity of the calculation, the link length ratios are considered instead of the specific values. Let

$$\frac{L_2}{L_3} = \alpha \quad \frac{L_3}{L_4} = \beta$$

Therefore, the final optimization design variable is $X = [\alpha, \beta]$

4.3. Constraints

a) Considering the structural requirements of the manipulator, the length ratio between adjacent links cannot be too large, that is,

$$X_{imin} \le X_i \le X_{i\max}, i = 1, 2$$

Where, X_{imin} , X_{imax} represent the minimum and maximum values of the design variables, which are set to 0.5 and 2, respectively.

b) The joint angles shall change within their motion ranges, i.e.

$$q_{jmin} \le q_j \le q_{j\max}, j = 2, 3, 4$$

Where, $q_{j\,\min}, q_{j\,\max}$ denote the minimum and maximum values of joint variables, and the values are shown in Table 1

c) This paper mainly considers the optimization under the condition that the total length of the link is fixed, that is,

$L = \sum_{k=1}^{n} L_k, n = 4$

d) Workspace constraint

The function of the manipulator is to complete the hedge trimming within the specified range, that is, the top and sides of the hedges within a range of 1-2 meters high and 0.8 meters wide. Suppose that in a very short period of time, the displacement of the tractor is zero, the manipulator should be able to reach any point in the cuboid with length, width and height of a, b and h, which is its target workspace, as shown in Fig. 1. So the target workspace needs to be a constraint.

4.4. Optimization Algorithm

The objective function and constraints have been determined above, and a suitable optimization algorithm needs to be used to obtain the optimal solution. Lim et al. proposed the Grey-based Taguchi method for optimization [24]. West et al. used genetic algorithm to optimize the structural parameters of a 7-DOF manipulator [25]. Taguchi method is mainly based on multiple experiments to collect data for optimization, which is too complicated. Genetic algorithm is widely used in structural parameter optimization of manipulators, but the convergence speed is slow and the calculation is complex. Different from this, particle swarm algorithm has no crossover and mutation, so it has low computational complexity and converges to the optimal solution faster. Therefore, this paper adopts particle swarm algorithm [26] to optimize the structural parameters of a 4-DOF manipulator.

5. Optimization Results

According to the input variables, optimization objectives, and constraints, the MATLAB optimization program is written, assuming that the size of particle swarm is 500 and the maximum iteration number is 300, the simulation results are shown in the following figures. Fig. 4 shows the initial state of the particles, the small red circles are randomly generated 500 points, representing the initial positions of 500 particles. Fig. 5 shows the change of particle position, selecting three positions of particles during the optimization process, from the Fig. 5 (a), (b), (c), it can be seen that with the increase of the iteration number, all particles continuously approach to the best position, and finally arrive, as shown in Fig. 6, this point is the target point to maximize the dexterity of the manipulator. Fig. 7 shows the convergence process during the iteration, it can be seen that the target point is reached at about the 25th iteration, and the convergence rate is faster.

According to the simulation results, the red point in Fig. 6 is the highest point on the entire surface, that is, the point with the maximum GCI, from the output of MATLAB, it can be seen that at this time, $L_2/L_3 = 1.27, L_3/L_4 = 1.48, \eta = 0.79521$, which are the optimal link length radios and the maximum GCI. According to the total arm length of the manipulator determined in section 2 and the length of L_1 is unchanged, it can be obtained that: $L_1 = 300\text{mm}, L_2 = 1190\text{mm}, L_3 = 937\text{mm}, L_4 = 633\text{mm}$. However, the link length radios before optimization are: $L_2/L_3 = 0.96, L_3/L_4 = 1.09$, submitting them into calculation formula of GCI, we can get $\eta = 0.68442$. Obviously, the optimized manipulator has a lager GCI. Section 4.1 shows that the lager the GCI is, the higher the dexterity of the manipulator will be. Therefore, the optimized manipulator is more dexterous.

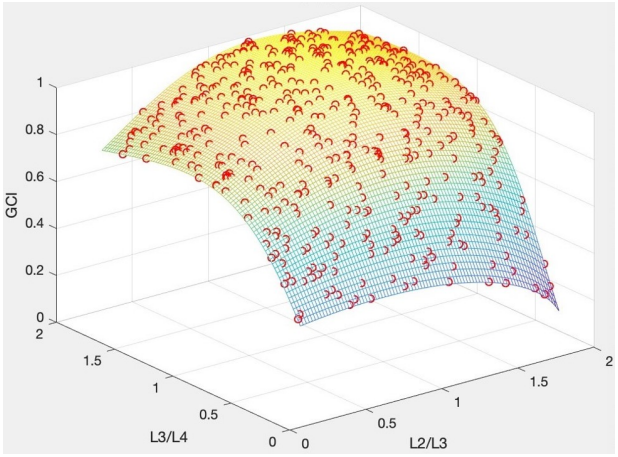

Fig. 4. Initial position status.

6. Simulation Verification of Manipulator Feasibility

In Section 4.3, the target workspace is taken as a constraint, so in the optimization algorithm, the random function is used to generate 10000 points in the target workspace and judge whether the manipulator can reach these points. If it can, the optimized link lengths meet the requirement and can be output. Considering that this constraint is to select points randomly, although the number of points is large, they are the discrete points of the workspace, which are still limited relative to the continuous workspace, so further verification is needed. This section verifies the feasibility of the optimized manipulator according to the optimal link lengths, that is, whether it meets the trimming requirements, using the method of workspace analysis, if the actual workspace covers the target workspace, it is proved that the optimized manipulator is feasible. Workspace is evaluated first, plenty of literature uses numerical methods. Cao et al. [27] used the Monte Carlo method in joint space to calculate the end point position according to forward kinematics to generate a 3D workspace. However, this

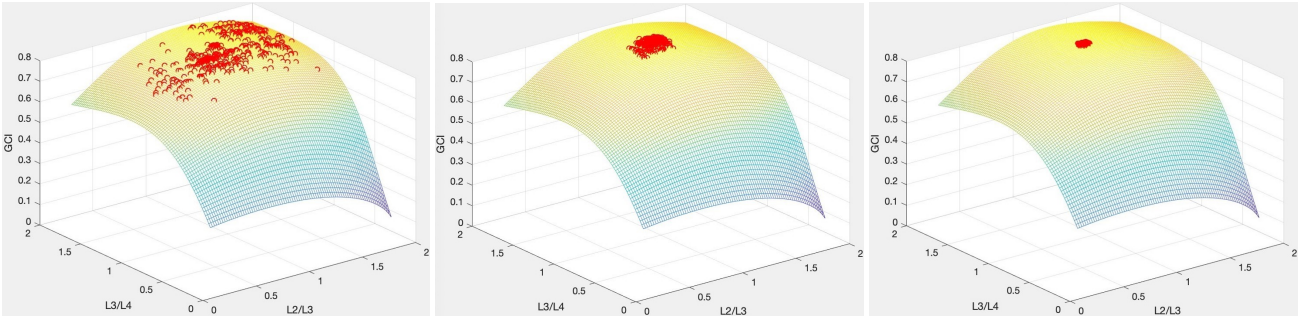

Fig. 5. (a) Position status 1; (b) Position status 2; (c) Position status 3.

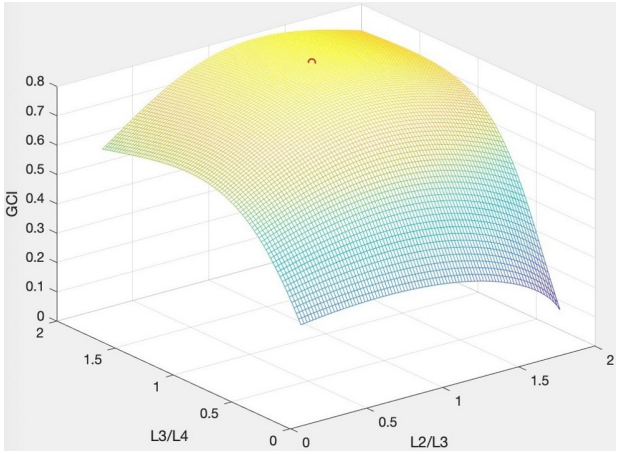

Fig. 6. Final status.

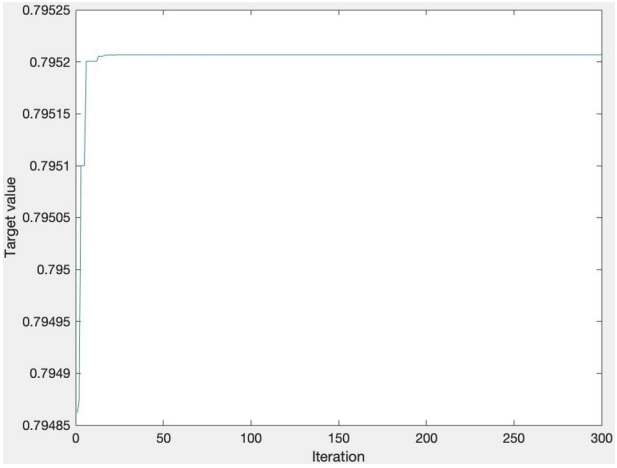

Fig. 7. Convergence process.

application of Monte Carlo method to joint space is not intuitive enough, and cannot directly demonstrate whether the manipulator can satisfy the trimming requirements. Contrary to above literature, this paper applies the Monte Carlo method in operating space. First, several 3D points are randomly generated in the target workspace, then the inverse kinematics algorithm is utilized to judge whether each point satisfies the range of joint variables and obtains the number of points in the reachable space. The degree of satisfaction is expressed by the percentage of reachability. The larger the percentage of points satisfied is, the better the reachability will be, if the reachability is 100%, the manipulator is feasible. Specific steps are as follows:

Step 1: First a 3 D space with a volume of V is defined, which is the target workspace for the manipulator, that is, $a \times b \times h$. In this space, the function Rand $(\mathrm{N}, 1)$ in MATLAB is utilized to generate uniform random 3D coordinate points with the size of N.

Step 2: In each cycle, randomly select a set of $3D$ coordinate points.

Step 3: Apply the inverse kinematics algorithm to obtain the joint variable θ_1. If θ_1 is within the motion range, go to step 4, otherwise return to step 2.

Step 4: Apply the inverse kinematics algorithm to calculate the joint variable θ_2 for the points that satisfy step 3 . If it is within the required range, go to step 5, otherwise return to step 2.

Step 5: Calculate θ_3, θ_4 by analogy. Get all 3D coordinate points that make $\theta_1, \theta_2, \theta_3, \theta_4$ within the motion ranges, and the number is recorded as N_0

Therefore, reachability can be expressed as

$$\lambda = (N_0/N) \times 100\% \tag{14}$$

The workspace of the manipulator before and after the optimization are simulated, and 10000 points are randomly generated in the target workspace. The workspace before and after the optimization are shown in Fig. 8,9. Among them, the red points represent 10000 randomly generated points, that is, the points in the target workspace, and the green points represent the points in the reachable space of the manipulator, that is, the points in the actual workspace.

Table 3. The comparison of link length and reachability.

State	L_1 / m m	L_2/*mm*	L_3 / m m	L_4 / m m	Number of red points	Number of green points	Reachability λ
Before	300	920	960	880	10000	8879	88.79 %
After	300	1190	937	633	10000	10000	100 %

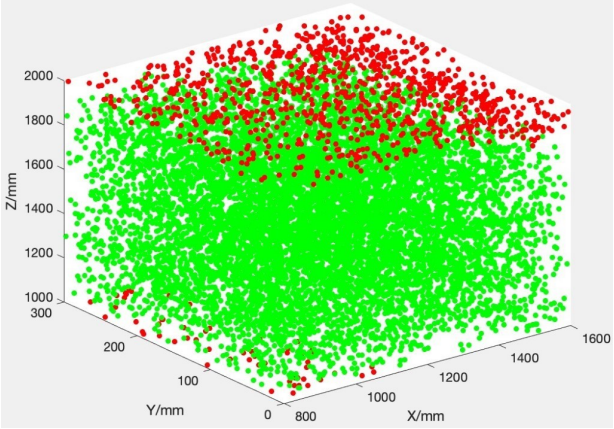

Fig. 8. Initial workspace.

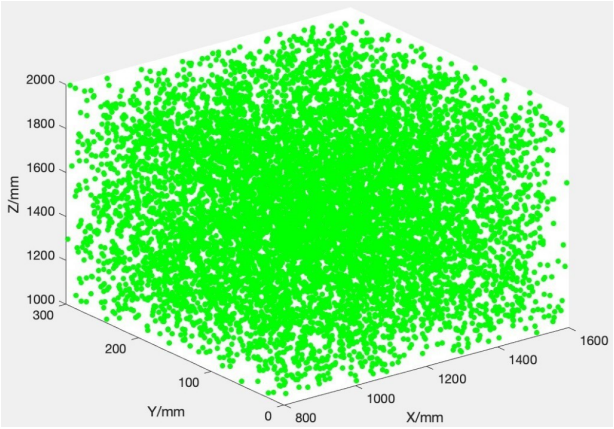

Fig. 9. Optimized workspace.

According to Fig. 8, 9, it can be seen that before optimization, the manipulator cannot fully reach the target workspace, there are still partially red unreachable points. After optimization, the green points all cover the red points. Table 3 is the comparison of link lengths and reachability of the manipulator before and after optimization. From that, it can be seen that the reachability of the manipulator before optimization is only 88.79%, while after optimization is 100%, improving by 11.21%, so the optimized manipulator is completely feasible.

7. Conclusion

(1) According to the trimming requirements, a 4-DOF trimming manipulator is designed. The D-H method is used to establish the coordinate frame of each link, then the forward kinematics equation is deduced, the inverse kinematics is solved by algebraic method, and the Jacobian matrix is obtained through the velocity mapping relationship.
(2) In order to obtain a higher dexterity, the structural parameter optimization model is established with the optimal GCI as the objective function, the link length ratios as the optimization variables, the joint angle ranges, the variable ranges, the total link length and the workspace as the constraints, and the particle swarm algorithm is used to solve the problem. The optimal link lengths (big arm, middle arm forearm) of the manipulator are 1190, 937, and 633mm, the initial GCI is 0.68442, the optimized GCI is 0.79521, which proves that the optimized manipulator has higher dexterity.
(3) In order to verify the feasibility of the optimized manipulator, this paper proposes a method to evaluate the workspace using Monte Carlo method in the operating space. Unlike other literature that evaluates it in joint space, this method is more intuitive. The reachability is used to express the degree to which the actual work space satisfies the target workspace. MATLAB simulation results show that the reachability of the optimized manipulator is 100%. It is proved that the optimized manipulator is completely feasible.

Acknowledgement

The work was supported by the Key R&D Program of Jiangsu Province (No:BE2018343). The authors would like to thank Mr. Lin Zhong, Chief Engineer, Sichuan Chuanlong Tractors Co. Ltd. (Chengdu, Sichuan, China), for their valuable suggestions and help.

References

[1] Q Wei. Research and design of double-sided high-efficiency hedge trimmer. *Guangxi: Guangxi University*, 2014.

[2] YJ Wang. Structural parameters optimization of multi-degree-of-freedom manipulator. *Beijing: Beijing Institute of Technology*, 2016.

[3] X W Wang, M H Wu, and J Zhou. Optimization and simulation of structural parameters of manipulators for high-quality tea picking robots. *Journal of Chinese Agricultural Mechanization*, 39(7):84–89, 2018.

[4] Haibo Tian, Hongwei Ma, and Juan Wei. Workspace and structural parameters analysis for manipulator of serial robot. *Nongye Jixie Xuebao/Transactions of the Chinese Society for Agricultural Machinery*, 44(4):196–201, 2013.

[5] JK Salisbury and JJ Craig. Articulated hands: Kinematic and force control issues. *The International Journal of Robotics Research*, 1(1):4–17, 1982.

[6] J. Angeles. A global performance index for the kinematic optimization of robotic manipulators. *Journal of Mechanical Design, Transactions of the ASME*, 113(3):220–226, sep 1991.

[7] G Tang. Research on kinetic characteristics of expressway hedgerow pruning robot. *Chongqing: Chongqing Jiaotong University*, 2018.

[8] Zhizhong Liu, Hongyi Liu, Zhong Luo, and Xiuheng Zhang. Improvement on Monte Carlo method for robot workspace determination. *Nongye Jixie Xuebao/Transactions of the Chinese Society for Agricultural Machinery*, 44(1):230–235, jan 2013.

[9] R P Ye. Research on modeling and simulation of 5-DOF serial manipulator. *Shenzhen: Shenzen University*, 2016.

[10] Geoffrey Pond and Juan A. Carretero. Quantitative dexterous workspace comparison of parallel manipulators. *Mechanism and Machine Theory*, 42(10):1388–1400, oct 2007.

[11] Mengke Qu, Hongbo Wang, and Yu Rong. Design of 6-DOF parallel mechanical leg of wheel-leg hybrid quadruped robot. *Nongye Gongcheng Xuebao/Transactions of the Chinese Society of Agricultural Engineering*, 33(11):29–37, 2017.

[12] Yu Rong, Zhenlin Jin, and Bingyan Cui. Configuration analysis and structure parameter design of six-leg agricultural robot with parallel-leg mechanisms. *Nongye Gongcheng Xuebao/Transactions of the Chinese Society of Agricultural Engineering*, 28(15):9–14, 2012.

[13] Lung Wen Tsai and Sameer Joshi. Kinematics and optimization of a spatial 3-UPU parallel manipulator. *Journal of Mechanical Design, Transactions of the ASME*, 122(4):439–446, 2000.

[14] H F Wang, B Yin, and R J Luo. Mechanism design and kinematics analysis of 4-dof SCARA robot system. *Journal of Mechanical & Electrical Engineering*, 36(12):1320–1324, 2019.

[15] Arkadeep Narayan Chaudhury and Ashitava Ghosal. Optimum design of multi-degree-of-freedom closed-loop mechanisms and parallel manipulators for a prescribed workspace using Monte Carlo method. *Mechanism and Machine Theory*, 118:115–138, 2017.

[16] Z Cai and B Xie. Robotics. *Third Edition, Beijing: Tsinghua University Press*, pages 8–9, 2015.

[17] J Song. Optimization design and simulation on structure parameter of eggplant picking robot. *Mechanical Design & Manufacture*, (6):166–168, 2008.

[18] J Wei. Design and Research of Hedge Seedling Pruning Manipulator. *Guangxi: Guangxi University*, 2013.

[19] H Z Li, Z G Hu, and L J Guo. Simulation study of manipulator with three degree of freedom. *Mechanical Design & Manufacture*, (10):186–189, 2014.

[20] Y D Fu. The design and research of mechanism and control system of the cucumber harvesting manipulator. *Jilin, Jilin University*, 2016.

[21] Tuomo Kivelä, Jouni Mattila, and Jussi Puura. A generic method to optimize a redundant serial robotic manipulator's structure. *Automation in Construction*, 81:172–179, 2017.

[22] Serdar Küçük and Zafer Bingül. Robot workspace optimization based on the global conditioning index. In *IFAC Proceedings Volumes*, volume 36, pages 117–122. IFAC Secretariat, 2003.

[23] Virendra Kumar, Soumen Sen, Shibendu S. Roy, Chandan Har, and S.N. Shome. Design Optimization of Serial Link Redundant Manipulator: An Approach Using Global Performance Metric. *Procedia Technology*, 14:43–50, 2014.

[24] Hyun Seop Lim, Soon Woong Hwang, Kyoo Sik Shin, and Chang Soo Han. Design optimization of the robot manipulator based on global performance indices using the grey-based taguchi method. In *IFAC Proceedings Volumes*, volume 43, pages 285–292, 2010.

[25] C. West, A. Montazeri, S. D. Monk, and C. J. Taylor. A genetic algorithm approach for parameter optimization of a 7DOF robotic manipulator. *International Federation of Automatic Control*, 49(12):1261–1266, 2016.

[26] Yi Ye, Chen Bo Yin, Yue Gong, and Jun jing Zhou. Position control of nonlinear hydraulic system using an improved PSO based PID controller. *Mechanical Systems and Signal Processing*, 83:241–259, jan 2017.

[27] Yi Cao, Haihe Zang, Lan Wu, and Tao Lu. An engineering-oriented method for the three dimensional workspace generation of robot manipulator. *Journal of Information and Computational Science*, 8(1):51–61, 2011.